Small icebergs space-time distribution around Greenland and Antarctica

Marine Laval, Jean Tournadre

Received 29th June 2019, Accepted 1st September 2019
First published on the web Xth XXXXXXXXXX 200X
DOI: 10.XXXX/XXXXXXXX

Surface and free-board of small icebergs (inferior to km^2), are for the first time accessible directly thanks to Cryosat-2, allowing to compute iceberg volumes. Measurements in Greenland, reveal two iceberg groups of specific free-board. Moreover each one have characteristic spatial distribution and varies with sea ice concentration. In Greenland and Antarctica, the evaluation of icebergs total volume spatial distribution, is close to the results we can found in scientific papers

1 Introduction

Antarctica (AN) and Greenland (GR) polar caps mass balance is negative, since the 1970s, and the mass deficit over last decade is multiply by 6 compared to 1970-1980 years [Mouginot et al.,2019, Rignot et al., 2019]. During 1970-2017 period, GR has contributed to 13.7 mm and AN to 14.0 mm to the sea level rise [Mouginot et al.,2019, Rignot et al., 2019].

Half of the mass loss in AN (1990-2010) come from iceberg calving, with $1321 \pm 144\,Gt/year$. The second half result of basal melting, with $1454 \pm 174\,Gt/year$ [Depoorter et al.,2013]. GR mass loss is $546 \pm 11\,Gt/year$ (2000-2012) [Benn et al.,2017]. This mass loss results from more processes than AN, surface melting and sub-glacial play an important role. Calving also contributes a lot to mass loss in GR [Enderlin et al., 2014]. A great part of ice caps mass loss is due to calving, this release of icebergs constitutes a fresh water flux toward ocean.

In AN, ice shelves fracturing, produce the majority (60-80%) of icebergs. These icebergs are generally larger and tabular than those in GR. They can measured until 10 000 km^2 (only 100-200 km^2 in GR) [Tournadre et al., 2016]. Larger icebergs carry the majority of volume, but smaller icebergs ($< 10\,km^2$) are responsible of melting and fresh water fluxes [Tournadre et al., 2016].

Few direct iceberg measurements are available, especially for small icebergs ($< 10\,km^2$). For these icebergs, Tournadre et al. [2008,2012] have developed a detection and analysis method from altimetry measurements. These icebergs have a characteristic signature inside the waveform measured by altimetry. Classical altimeters used, can only detect icebergs in free water (but can not in sea ice). Moreover iceberg surfaces and volumes are indirectly obtained by the method of Tournadre et al., [2012].

Cryosat-2 is the first altimeter to possess an interferometric (SARin) mode, which measured directly surfaces and free-boards in free water and sea ice. In this study Cryosat-2 data set was used to analyse surfaces, free-boards and volumes under sea ice concentration and back scattering, during 2010-2018, and their distributions were compared with other studies. However Cryosat-2 measurements are geographically limited to continental margin.

2 Methods

Iceberg volumes were obtained from surface and free-board measurements (Cryosat-2), with :

$$V_{tot} = \frac{V_e \rho_e}{\rho_e - \rho_g} \tag{1}$$

It draws on emerged volume $V_e = h_e S_e$, h_e is the free-board. Sea water density taken, is $\rho_e = 1025 kg.m^{-3}$, and iceberg density is the density of pure ice: $\rho_g = 917 kg.m^{-3}$.

Sea ice concentration used, is store by Cersat since 1992. It is calculated from Artist Sea Ice (ASI) algorithm, developed at Brenen university in Germany. ASI calculate a daily map of sea ice concentration with a resolution of 12.5 km. In this study icebergs in free water have sea ice concentration bellow 20%, and those in sea ice have a sea ice concentration above 20%. Lot of islands and rocks are along GR coast, which can increase false detection, thus I take only iceberg beyond 10 km.

Computation of free-board modes is done for free water, sea ice and total. Icebergs below a free-board threshold (GR all: 28.5 m, free: 24.2 m, sea ice: 31.5 m, AN all: 18.3 m, free: 17.5 m, sea ice: 18.5 m) form the first mode. The second mode includes icebergs over this threshold. Each mode receives a Gaussian adjustment, which provides the mean and standard deviation, used for the calculation of Gaussian PDF. Total PDF is the sum of normalized mode 1 and 2 PDFs.

3 Free-boards, surfaces and volumes

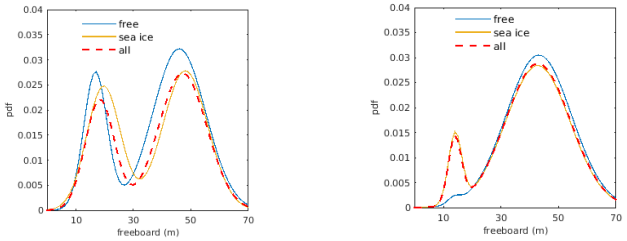

Fig. 1 Free-board PDF in GR (left) and AN (right)

Free-board distribution in GR and AN is bimodal. Each mode has (mostly) a Gaussian distribution.

In GR the first mode is between 10-28 m and the second mode between 35-60 m (Figure.1). In AN bimodal distribution is less visible. The first mode (10-17 m) is only present in sea ice, with a lower frequency (¡5%) than the second mode (30-60 m) (Figure.1). The first mode can be due to false detection.

In GR and AN 90% of icebergs are below 0.2 km^2. Surface distribution can be represented by power law: $P(x) = ax^b$. Power law are estimated from $\log P$ on $\log x$. All distribution, follow a power law with a slope of -2. A stronger slope than the one found (1.5) by Tournadre et al.[2016]. In GR icebergs in free water, have smaller surfaces, we don't find it in AN where the concentration doesn't have an influence on the distribution.

The majority of the icebergs (90%) in GR and AN has a volume below 0.1 km^3. Volume PDFs have the same form than surfaces PDFs, and are also power laws (report figure). Linear regression give a slope of -2, except for free water iceberg in GR (-1.5). Slopes are close to those found for surfaces, excepted in free water in GR, with a slope close to the one found by Tournadre et al.[2016].

4 Cross distributions: Back-scattering and free-board

For a better understanding of main parameters (free-board and volume), I studied the influence of the back scattering and the sea-ice concentration. In GR, two clusters are clearly recognizable. The first one, contains free-board between 5-32 m and back scattering from -4 to 9 dB. The second has free-board between 35-62 m and back scattering from -17 to -5 dB (Figure.2(a)). Cluster 2 is mostly inside sea ice (Figure.3(a)).

In AN, the distribution also shows two clusters: A dominant cluster 2, of 21-62 m free-board and back scattering from -17 to -3 dB, and a smaller cluster 1 of 10-20 m free-board and back scattering of -2 to 11 dB (Figure.2(b)). Contrary to GR,

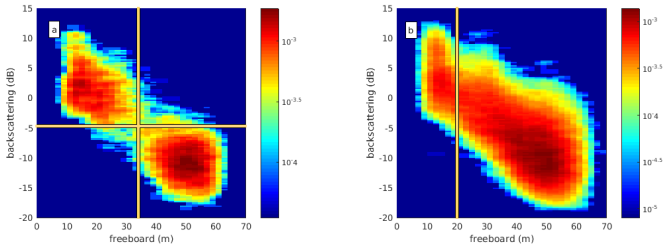

Fig. 2 (a) Joint distribution free-board and backscattering in GR and (b) in AN

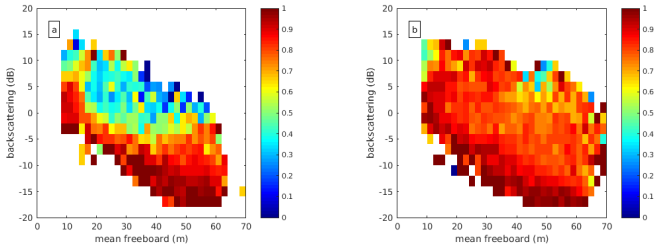

Fig. 3 (a) Likelihood distribution of sea ice (1 = sea ice, 0 = no sea ice) function of free-board and back scattering in GR and (b) AN

the two clusters are associated to the same sea ice conditions (Figure.3(b)). For the two clusters, lower back scattering are associated to a higher sea ice concentration (Figure.3(b)). It can indicate a increase of back scattering with the increase of the ambient temperature [Onstott and Gogineni, 1985].

5 Geographical distribution

In GR half of ice mass loss comes from northwest, central-west, and southeast coast. Central-east coast also contributes to the loss [Mouginot et al., 2019]. In AN, since 1979, the mass loss is divided in three region: eastern, western and AN peninsula [Rignot et al., 2013]. Before the 2010s, the main player of mass loss was eastern AN. However over the last decade, the mass loss is dominated by the western part (Amundsen and Bellingshausen sea) [Rignot et al.,2019].

The first GR cluster is divided in two groups, one of high back scattering in free water and the second of lower back scattering in sea ice. The first cluster group (lower free-board), is in northwestern (Kong Oscar glacier), central-western (Rink Isbrae glacier) and in southeastern part (Helheim glacier) (Figure.4(a)). The second group (lower free-board) and cluster 2 (higher free-board) are distributed in the eastern part and to the northwestern only for cluster 2 (Kong Oscar and Bowdoin glaciers) (Figure.4(b) and (c)). This distribution agree with the typical description of icebergs describe by Mouginot et al., [2019].In AN cluster 1 and 2 distribution are similar.

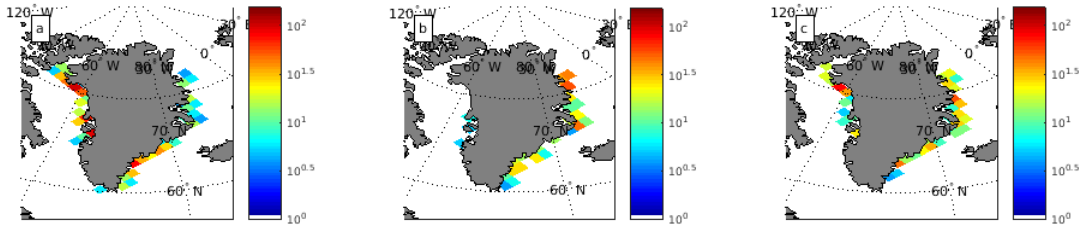

Fig. 4 GR spatial distribution of (a) cluster 1 in free water (b) sea ice and (c) cluster 2.

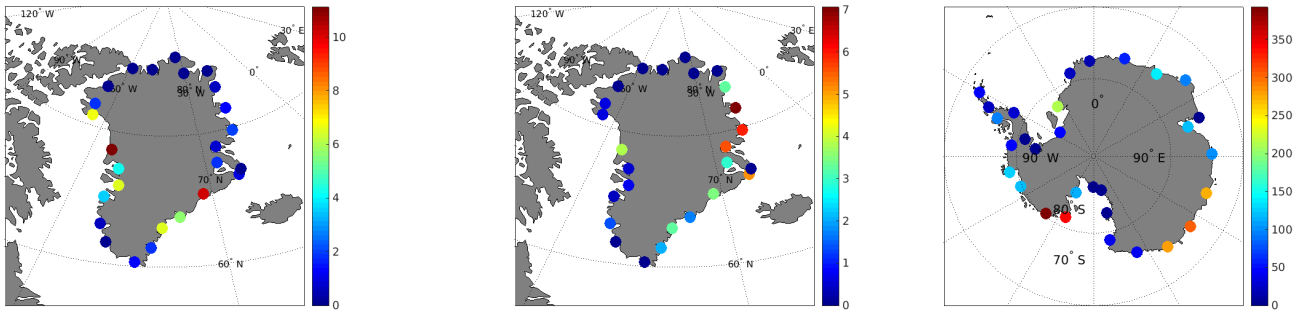

Fig. 5 GR Total volume (km^3) distribution in free water (left) and sea ice (middle). AN total volume (km^3) distribution (right)

For GR and AN, I use the Matlab coastline to determine for each iceberg the coast nearest point. Total volume along the coast is calculated by $V_t = \sum_{i=1}^{n} V_i$ ($n_G R = 500$ km and $n_A N = 1000$ km).

In GR, according to Mouginot and al. [2019] between 2010 and 2018, the higher ice losses by calving come from northwestern (30 Gt/year), southeastern (25 Gt/year), central-west (20 Gt/year) and central-east (13 Gt/year). We observe from the total volume computed, a loss in southeastern part, of 18 km^3 at Kangerlussuaq glacier, 12 and 10 km^3 around Helheim glacier, and inside northwestern sector (12 and 8 km^3). Free water icebergs contribute to the ice loss in northwestern sector (12 ans 7 km^3) and southeastern (11 and 9 km^3) (Figure.5). Icebergs in sea ice play a part on the ice loss in northeastern sector (between 6 and 7 km^3) (Figure.5).

In AN to 2009 from 2017, biggest mass loss come from western (132 $\pm$ 6 Gt/year), largely in Admundsen sea, and at the eastern (37 $\pm$ Gt/year) [Rignot et al.,2019]. From our volumes computed, larger volume losses, are in the western towards Bellingshaussen sea (350 and 300 km^3) (Figure.5). These volumes come from icebergs calved of northern glaciers (Pine Island, Getz and AN west Peninsula), drifting below coastal AN current. A few icebergs calve of AN West Peninsula, because mass loss is mainly basal at this place. On eastern, we found also largest volume loss (300 and 2x275 km^3) by Totten, Holmes or else Nonnis glaciers (Figure.5). Lastly volumes from Filchner ice shelves (220 km^3) are due to the re-distribution of northeast glaciers icebergs, by coastal AN current (Figure.5).

6 Conclusions

Cryosat-2 is the first altimeter, which allows icebergs detection in sea ice, and to collected the free-board and surface directly. These measures obtained allow to access to the volume of each iceberg.

The statistic analysis of free-board, shows in GR, 2 modes (18 and 38 m on average). In free water, small free-board and volume icebergs, thus higher back scattering, are melting indicator. In AN free-board distribution is not bimodal, but Gaussian, reflect flatter icebergs.

Joint analysis of free-board and back scattering, shows two different clusters in GR and only one in AN. In GR, clusters depend of sea ice concentration unlike in AN. Moreover the two clusters in GR have a particular geographical distribution. To go further in the study, we should compare the free-board with the ice thickness.

Total volume distribution in GR, reveal an important mass loss by calving around emissary glaciers. In AN, larger ice volume calve at the western part. Mass losses distribution in

GR and AN match with result found by Rignot et al. [2019], et Mouginot et al. [2019].

Acknowledgments

References

Douglas I. Benn, Tom Cowton, Joe Todd, and Adrian Luckmann. Glacier calving in greenland. ***Current Climate Change Reports***, 3(4):282 290, Dec 2017. ISSN 2198-6061. doi: 10.1007/s40641-017-0070-1. URL https:/doi.org/10.1007/s40641-017-0070-1.

M. A. Depoorter, J. L. Bamber, J.A Griggs, J. T. M Lenaerts, S.R.M Ligtenberg, M.R van den Broeke and G. Moholdt. Calving fluxes and basal melt rate of Antarctic ice shelves. ***Nature***, 502, 2013. doi:10.1038/nature12567.

Ellyn M. Enderlin, Ian M. Howat, Seongsu Jeong, Myoung-Jong Noh, Jan H. van Angelen, and Michiel R. van den Broeke. An improved mass budget for greenland ice sheet. ***Geophysical Research Letters***, 41(3):866 872, 2014. ISSN 1944-8007. doi: 10.1002/2013GL059010. URL https:/dx.doi.org/10.1002/2013GL059010.

Jérémie Mouginot, Eric Rignot, Anders A. Bjork, Michiel van den Broeke, Romain Millan, Mathieu Morlighem, Brice Noël, Bernd Scheuchl, and Michael Wood. Forty-six years of Greenland Ice Sheet mass balance from 1972 to 2018. ***Proceeding of the National Academy of Sciences***, 116(19):9239 9244, 2019. ISSN 0027-8424. doi: 10.1073/pnas.1904242116. URL https://www.pnas.org/content/116/19/9239

Eric Rignot, Jérémie Mouginot, Bernd Scheuchl, Michiel van den Broeke, Melchior J. van Wessem, and Mathieu Morlighem. Four decades of antarctic ice sheet mass balance from 1979 2017. ***Proceedings of the National Academy of Sciences***, 116(4):1095 1103, 2019. ISSN 0027-8424. doi: 10.1073/pnas.1812883116. URL https://www.pnas.org/content/116/4/1095.

J. Tournadre, K. Whitmer, and F. Girard-Ardhuin. Iceberg detection in open water by altimeter waveform analysis. ***J. Geophys. Res.***, 113(C8):C08040, AUG 23 2008. ISSN 0148-0227. doi: 10.1029/2007JC004587.

J. Tournadre, F. Girard-Ardhuin, and B. Legresy. Anatrctic icebergs distributions, 2002-2010. ***J. Geophys. Res.***, 117:C05004, MAY 1 2012. ISSN 0148-0227. doi: 10.1029/2011JC007441.

J. Tournadre, N. Bouhier, F. Girard-Ardhuin, and F. Remy. Antarctic icebergs distributions 1992-2014. ***J. Geophys. Res.***, 121(1):327 349, JAN 2016. ISSN 2169-9275. doi: 10.1002/2015JC011178.